International Journal of Computational Engineering Science
Vol. 3, No. 1 (2002) 73–87

SCALAR MIXING AND CHEMICAL REACTION SIMULATIONS USING LATTICE BOLTZMANN METHOD

HUIDAN YU

Department of Aerospace Engineering, Texas A&M University, College Station, Texas 77843-3141

LI-SHI LUO

ICASE, Mail Stop 132C, NASA Langley Research Center, 3 West Reid Street, Building 1152, Hampton, Virginia 23681-2199

SHARATH S. GIRIMAJI

Department of Aerospace Engineering, Texas A&M University, College Station, Texas 77843-3141

We simulate scalar mixing and chemical reactions using the lattice Boltzmann method. Simulations of initially non-premixed binary mixtures yield scalar probability distribution functions that are in good agreement with direct numerical simulation (of Navier-Stokes equation) data. One-dimensional chemically-reacting flow simulation of a premixed mixture yields a flame speed that is consistent with experimentally determined value. These results serve to establish the feasibility of the lattice Boltzmann method as a viable tool for computing turbulent combustion.

1. Introduction

The lattice Boltzmann equation (LBE) method is emerging as a physically accurate and computationally viable tool for simulating laminar and turbulent flows.[1–7] On the theoretical front, rigorous mathematical proof now exists demonstrating that the lattice Boltzmann method (LBM) is a special finite difference scheme of the Boltzmann equation that governs all fluid flows.[4] (Recall that the Navier-Stokes equation also has its basis in the Boltzmann equation.) It has also been shown that LBM can be related to some conventional computational fluid dynamics methods and the proof brings to light the advantages of the LBM.[8,9] Detailed numerical studies with the LBM demonstrate the physical accuracy and computational viability for solving complex fluid flow problems.[2,3,10,11]

With few notable exceptions, the LBM has been so far used mostly for single-component, inert and isothermal flows. In this paper, we simulate scalar mixing in

a multi-component flow and a chemical reacting flow using the lattice Boltzmann computational approach. At the continuum level, the mixing example considered appears as a pure diffusion problem without any advection velocities. However, at the mesoscopic level, each of the components is associated with non-zero velocities. Hence, the problem considered is truly more significant than simple passive scalar mixing. Due to the kinetic nature of the LBE scheme, the extension of this method to cases with non-trivial macroscopic velocity field is straight forward. The second problem considered is one-dimensional flame propagation in a well-stirred homogeneous mixture of propane and air. The flame speed calculated using the LBM is in good agreement with experimental data. This problem is very similar to the one solved by Yamamoto[15] but with a sightly different physical field. The overall results are encouraging and establish the feasibility of the LBM as a viable computational approach for simulating mixing and reaction.

The remainder of the paper is organized as follows. In Section 2, the lattice Boltzmann equations used in the simulations are presented. The results from the mixing and reacting simulations are presented in Section 3. We conclude in Section 4 with a brief discussion. Details of the physical parameters used in the reacting flow simulation are presented in Appendix A.

For an introduction to the LBM, the reader is referred to a recent review by Chen and Doolen.[10]

2. Lattice Boltzmann Equations

The basic LBE[1] for a single-component medium consists of two basic steps: collision and advection. The particle distribution function is thermalized locally through collision processes and advection to the closest neighboring sites occurs according to a small set of discrete particle velocities. The LBE proposed here is the lattice Boltzmann scheme with BGK approximation[12,13]

$$n_\alpha(\boldsymbol{x}+\boldsymbol{e}_\alpha\delta_t, t+\delta_t) = n_\alpha(\boldsymbol{x},t) - \frac{1}{\tau}[n_\alpha(\boldsymbol{x},t) - n_\alpha^{(\mathrm{eq})}(\boldsymbol{x},t)] \tag{1}$$

where n_α is the number density distribution function with discrete velocity $\boldsymbol{e}_\alpha$, $n_\alpha^{(\mathrm{eq})}$ is the equilibrium distribution function and τ is the relaxation time (towards equilibrium) which determines the viscosity. The time-step size is δ_t, which is the time taken for the advection process to be completed. For the sake of simplicity without losing generality, we adopt the nine-velocity model (D2Q9), as shown in Fig. 1. Then the equilibrium distribution function for isothermal fluids is given as

$$n_\alpha^{(\mathrm{eq})} = w_\alpha n\,[1 + \frac{1}{c_s^2}(\boldsymbol{e}_\alpha\cdot\boldsymbol{u}) + \frac{1}{2c_s^4}(\boldsymbol{e}_\alpha\cdot\boldsymbol{u})^2 - \frac{1}{c_s^2}u^2] \tag{2}$$

in which the discrete particle velocities $\boldsymbol{e}_\alpha$ and the weighting factor w_α ($\alpha = 0,1,2,\cdots,8$) are

$$\boldsymbol{e}_\alpha = \begin{cases} (0,0), & \alpha = 0 \\ (\cos[(\alpha-1)\pi/2], \sin[(\alpha-1)\pi/2]), & \alpha = 1,2,3,4 \\ (\cos[(\alpha-5)\pi/2+\pi/4], \sin[(\alpha-5)\pi/2+\pi/4]), & \alpha = 5,6,7,8 \end{cases} \tag{3}$$

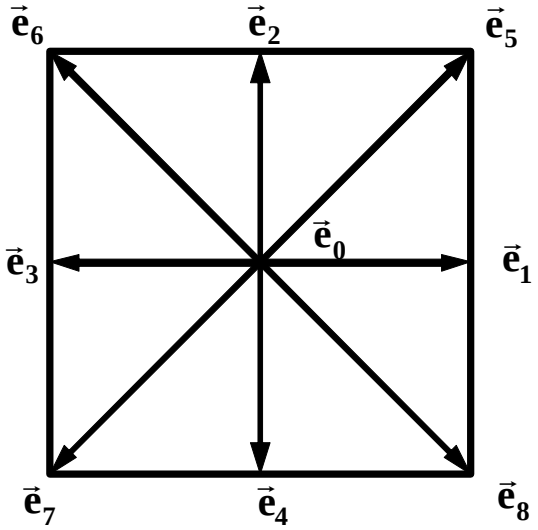

Fig. 1. D2Q9 model. Nine discrete velocities on a square lattice.

and

$$w_\alpha = \begin{cases} 4/9, & \alpha = 0 \\ 1/9, & \alpha = 1,2,3,4 \\ 1/36, & \alpha = 5,6,7,8 \end{cases} \tag{4}$$

respectively. The sound speed is $c_s = 1/\sqrt{3}\,(\delta_x/\delta_t)$ with δ_x being the lattice constant of the underlying square lattice. The macroscopic quantities, such as particle density n, mass density ρ and mass velocity $\boldsymbol{u}$ are given by

$$n = \sum_\alpha n_\alpha \tag{5}$$

$$\rho = mn \tag{6}$$

$$\rho \boldsymbol{u} = m \sum_\alpha n_\alpha \boldsymbol{e}_\alpha \tag{7}$$

where m is the molecular weight.

2.1. *Lattice Boltzmann equations for scalar mixing*

Consider a multi-species field: n_α^σ denotes the number density distribution function of a particular species σ with discrete velocity $\boldsymbol{e}_\alpha$, $\sigma = 1,2,3,\cdots$. The number density and molecular weight of species σ are given respectively by n^σ and m^σ. Then mass density of the σ-species is given as

$$\rho^\sigma = m^\sigma n^\sigma = m^\sigma \sum_\alpha n_\alpha^\sigma \tag{8}$$

Number density, mass density and velocity of the mixture are

$$n = \sum_\sigma n^\sigma \tag{9}$$

$$\rho = \sum_\sigma \rho^\sigma \tag{10}$$

and

$$\boldsymbol{u} = \frac{1}{\rho}\sum_\sigma (m^\sigma \sum_\alpha n_\alpha^\sigma \boldsymbol{e}_\alpha) \tag{11}$$

respectively.

For the sake of concreteness and simplicity without losing generality, we construct a LBE for binary mixture with $\delta_x = \delta_t = 1$. Let σ and ς denote the two species of interest. The LBE for each species is

$$n_\alpha^\sigma(\boldsymbol{x} + \boldsymbol{e}_\alpha, t+1) = n_\alpha^\sigma(\boldsymbol{x}, t) + \Omega_\alpha^\sigma(\boldsymbol{x}, t) \tag{12}$$

where the collision operator

$$\Omega_\alpha^\sigma = -\frac{1}{\tau^\sigma}[n_\alpha^\sigma - n_\alpha^{\sigma(\mathrm{eq})}] + \frac{J_\alpha^{\sigma\varsigma}}{m^\sigma} \tag{13}$$

includes an additional term $J_\alpha^{\sigma\varsigma}$ which reflects interactions between two species.

We use the following number density equilibrium distribution function

$$n_\alpha^{\sigma(\mathrm{eq})} = w_\alpha n^\sigma[1 + 3(\boldsymbol{e}_\alpha \cdot \boldsymbol{u}') + \frac{9}{2}(\boldsymbol{e}_\alpha \cdot \boldsymbol{u}')^2 - \frac{1}{2}u'^2] \tag{14}$$

with

$$\boldsymbol{u}' = \frac{1}{\rho}\sum_\sigma \frac{m^\sigma}{\tau^\sigma}(n^\sigma \boldsymbol{u}^\sigma) \tag{15}$$

The binary interaction term is modeled as[14]

$$J_\alpha^{\sigma\varsigma} = \frac{1}{\tau^{\sigma\varsigma}} n_\alpha^{eq} \cdot [\nabla x^\sigma + (x^\sigma - \omega^\sigma)\frac{\nabla\rho}{\rho}] = -J_\alpha^{\varsigma\sigma} \tag{16}$$

where x^σ and ω^σ are molar and mass fractions of the species σ

$$x^\sigma = \frac{n^\sigma}{n}, \quad \omega^\sigma = \frac{\rho^\sigma}{\rho}$$

and

$$n_\alpha^{(\mathrm{eq})} = w_\alpha n[1 + 3(\boldsymbol{e}_\alpha \cdot \boldsymbol{u}) + \frac{9}{2}(\boldsymbol{e}_\alpha \cdot \boldsymbol{u})^2 - \frac{1}{2}u^2] \tag{17}$$

2.2. *Lattice Boltzmann Equations for Reacting flow*

Here we simulate simple one-dimensional flame propagation through a premixed mixture of propane and air. The problem studied is identical to that of Yamamoto[15] but the physical combustion field is sightly different. The simplifying assumptions invoked in this study are now listed:

- No external forces in the field and the flow is incompressible.
- The chemical reaction (heat release) does not affect the flow field; temperature and concentration fields are decoupled and solved separately.
- Nitrogen is inert.
- The transport properties are constants (not functions of temperature).
- Viscous energy dissipation and radiative heat losses are negligible.
- Simple one step reaction is considered

  $$C_3H_8 + 5O_2 \Rightarrow 3CO_2 + 4H_2O$$

  and the over-all reaction rate is given by

  $$\omega_{\rm ov} = \kappa_{\rm ov} C_{C_3H_8} C_{O_2} e^{-E/RT}$$

  where $C_{C_3H_8}$, C_{O_2}, $\kappa_{\rm ov}$ and E are concentrations of fuel propane and oxygen, reaction coefficient and effective activation energy respectively.

In a reacting flow, the state of the fluid at any given point in space and time can be completely specified in terms of fluid velocity, composition vector (either in terms of mass fraction or concentration) and temperature. We will need to develop the LBE for all these variables. For generating a background flow, the conventional LBM sub-steps of collision (relaxation) and streaming (convection) are used. However for the temperature and concentration fields, there is an extra sub-step between collision and streaming sub-steps to account for reaction. This is identical to the time-splitting approach used in continuum methods for chemically reacting flows.

Flow field. The background flow-field is obtained using the following stencil for partial pressure

$$p_\alpha(\boldsymbol{x} + \boldsymbol{e}_\alpha, t+1) = p_\alpha(\boldsymbol{x}, t) - \frac{1}{\tau_p}[p_\alpha(\boldsymbol{x}, t) - p_\alpha^{(\rm eq)}(\boldsymbol{x}, t)] \tag{18}$$

where

$$p_\alpha^{(\rm eq)} = w_\alpha p[1 + 3(\boldsymbol{e}_\alpha \cdot \boldsymbol{u}) + \frac{9}{2}(\boldsymbol{e}_\alpha \cdot \boldsymbol{u})^2 - \frac{3}{2}u^2] \tag{19}$$

The total pressure p($= \rho c_s^2$) and the fluid velocity are calculated using

$$p = \sum_\alpha p_\alpha$$

$$\boldsymbol{u} = \frac{1}{p}\sum_\alpha \boldsymbol{e}_\alpha p_\alpha$$

This is the velocity used for determining the equilibrium distribution functions in temperature and concentration fields.

Temperature and concentration fields. For temperature (T is normalized by $T_c = E/R$) and concentration (mass ratio Y^i, $i \in \{C_3H_8,\ O_2,\ CO_2,\ H_2O\}$) fields, there is an extra computational sub-step, reaction, besides conventional computational sub-steps of collision and advection.

- COLLISION

$$\tilde{T}_\alpha(\boldsymbol{x},t) = T_\alpha(\boldsymbol{x},t) - \frac{1}{\tau_T}[T_\alpha(\boldsymbol{x},t) - T_\alpha^{(\mathrm{eq})}(\boldsymbol{x},t)] \tag{20}$$

$$\tilde{Y}_\alpha^i(\boldsymbol{x},t) = Y_\alpha^i(\boldsymbol{x},t) - \frac{1}{\tau_i}[Y_\alpha^i(\boldsymbol{x},t) - Y_\alpha^{i(\mathrm{eq})}(\boldsymbol{x},t)] \tag{21}$$

where

$$T_\alpha^{(\mathrm{eq})} = w_\alpha T[1 + 3(\boldsymbol{e}_\alpha \cdot \boldsymbol{u}) + \frac{9}{2}(\boldsymbol{e}_\alpha \cdot \boldsymbol{u})^2 - \frac{3}{2}u^2] \tag{22}$$

$$Y_\alpha^{i(\mathrm{eq})} = w_\alpha Y^i[1 + 3(\boldsymbol{e}_\alpha \cdot \boldsymbol{u}) + \frac{9}{2}(\boldsymbol{e}_\alpha \cdot \boldsymbol{u})^2 - \frac{3}{2}u^2] \tag{23}$$

and

$$T = \sum_\alpha T_\alpha, \qquad Y^i = \sum_\alpha Y_\alpha^i$$

Relaxation time-constant τ_T is determined by thermal diffusivity and τ_i's are determined by the diffusivity of corresponding species.

- REACTION

Reaction equation

$$C_3H_8 + 5O_2 \rightarrow 3CO_2 + 4H_2O$$

$$\omega_{\mathrm{ov}} = \kappa_{\mathrm{ov}} \tilde{C}_{C_3H_8} \tilde{C}_{O_2} e^{-1/\tilde{T}}$$

Concentrations

$$\tilde{C}_i = \rho \tilde{Y}_i / M_i$$

Reaction terms

$$Q_{Y^i} = \lambda_i \frac{M_i t_0}{\rho} \omega_{\mathrm{ov}}$$

$$Q_T = \frac{Q t_0}{\rho c_p T_c} \omega_{\mathrm{ov}}$$

where

$$\tilde{Y}^i = \sum_\alpha \tilde{Y}_\alpha^i, \quad \tilde{T} = \sum_\alpha \tilde{T}_\alpha$$

In the above equations, the stoichiometric coefficients (λ's) for the various species are: $\lambda_{C_3H_8} = -1$, $\lambda_{O_2} = -5$, $\lambda_{CO_2} = 3$, $\lambda_{H_2O} = 4$ and all physical parameters are listed in Appendix A.

- STREAMING

$$T_\alpha(\boldsymbol{x}+\boldsymbol{e}_\alpha, t+1) = \tilde{T}_\alpha(\boldsymbol{x}, t) + w_\alpha Q_T$$

$$Y^i_\alpha(\boldsymbol{x}+\boldsymbol{e}_\alpha, t+1) = \tilde{Y}^i_\alpha(\boldsymbol{x}, t) + w_\alpha Q_{Y^i}$$

3. Simulations

As mentioned in the introduction, the primary objective of this work is to investigate the ability of the LBM to simulate scalar mixing, chemical reaction and ultimately turbulent combustion. Working towards this end, we perform simulations of two unit problems: one to establish the mixing characteristics and another to demonstrate the chemical reaction scheme.

3.1. *Non-premixed binary scalar mixing*

This problem epitomizes the scalar mixing issues encountered in a typical non-premixed combustion application. Two species (presumably fuel and oxidizer) are initially segregated and randomly distributed in the computational domain which in the present case is a square box. Mesh size is set 500×500. The two species are generically labelled as black and white. A typical initial distribution is shown in Figure 2.

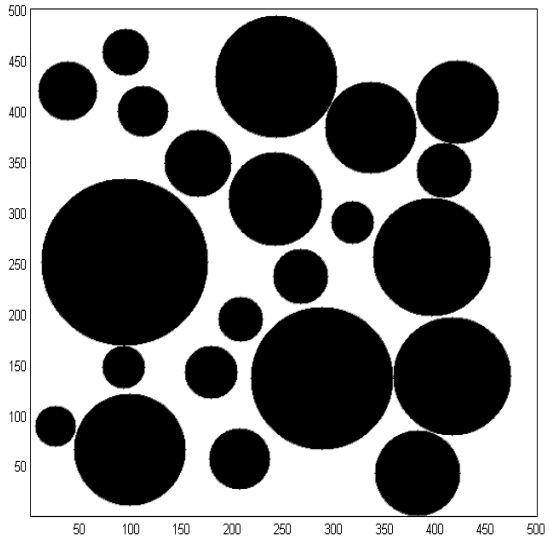

Fig. 2. Initial number density distribution for both equal and unequal mass cases.

The macroscopic velocity is set everywhere to zero corresponding to a pure diffusion problem. It should be reiterated here that the mesoscopic velocities are

non-zero. The initial values for the number densities are $n^b = 1.0$, $n^w = 0.0$ in region of the black species and $n^w = 1.0$, $n^b = 0.0$ in region of white species. Simulations are performed for two different sets of relaxation time scales: $\tau^b = \tau^w = 1.0$ and $\tau^{bw} = \tau^{wb} = 30.0$. Citing homogeneity of the scalar field, periodic boundary conditions are used in all directions.

To discretize ∇x^σ and $\nabla \rho$ in the binary interaction term in Equation 16, we use central difference operator. Taylor series expansion of each of $f(\boldsymbol{x} + \boldsymbol{e}_i)$ terms to the second order leads the following stencil of ∂_x and ∂_y:

$$\partial_x = \frac{1}{12}\begin{bmatrix} -1 & 0 & 1 \\ -4 & 0 & 4 \\ -1 & 0 & 1 \end{bmatrix}, \quad \partial_y = \frac{1}{12}\begin{bmatrix} 1 & 4 & 1 \\ 0 & 0 & 0 \\ -1 & -4 & -1 \end{bmatrix} \tag{24}$$

That is

$$\partial_x f(\boldsymbol{x}) \approx \frac{1}{12}[4f(\boldsymbol{x}+\boldsymbol{e}_1)+f(\boldsymbol{x}+\boldsymbol{e}_5)+f(\boldsymbol{x}+\boldsymbol{e}_8)-f(\boldsymbol{x}+\boldsymbol{e}_6)-4f(\boldsymbol{x}+\boldsymbol{e}_3)-f(\boldsymbol{x}+\boldsymbol{e}_7)] \tag{25}$$

$$\partial_y f(\boldsymbol{x}) \approx \frac{1}{12}[4f(\boldsymbol{x}+\boldsymbol{e}_2)+f(\boldsymbol{x}+\boldsymbol{e}_5)+f(\boldsymbol{x}+\boldsymbol{e}_6)-f(\boldsymbol{x}+\boldsymbol{e}_7)-4f(\boldsymbol{x}+\boldsymbol{e}_4)-f(\boldsymbol{x}+\boldsymbol{e}_8)] \tag{26}$$

in which f can be x^σ and ρ^σ.

The lattice Boltzmann methodology permits simulation of mixing between species of equal or unequal number and mass densities with equal facility. However, in continuum based methods, mixing between species of unequal mass densities is not straight-forward. This represents a fundamental advantage of the LBM over continuum-based methods.

Equal mass case ($m^b = m^w = 1.0$). The first case studied is mixing of two fluids of equal molecular weights and number densities, hence of equal mass density. This case is particularly interesting as the results can be directly compared with directed numerical simulation (DNS) of Navier-stokes equation data of Eswaran and Pope.[16] In this case, the number density and mass density are equivalent since the molecular weight of the two species are identical.

Figure 3(a) shows the time evolution of the probability density function(pdf) of scalar $\overline{\rho}$:

$$\overline{\rho} = \frac{\rho^b - \rho^w}{\rho^b + \rho^w}$$

The corresponding DNS[16] data is shown in Figure 3(b). The LBE and DNS data show excellent qualitative agreement. In particular, the change of the pdf shape from the initial double-delta shape through a nearly uniform distribution to, finally, a Gaussian-like distribution is well captured by the LBE results. It deserves mention here that many other mixing models do not, even qualitatively, capture the form of pdf during evolution.

In Figure 4, the time evolution of the root-mean-square (rms) of scalar fluctuations (ρ') obtained from LBE is compared with that from DNS:[16]

$$\rho' = \sqrt{\langle(\rho^b - \langle\rho^b\rangle)^2\rangle} \tag{27}$$

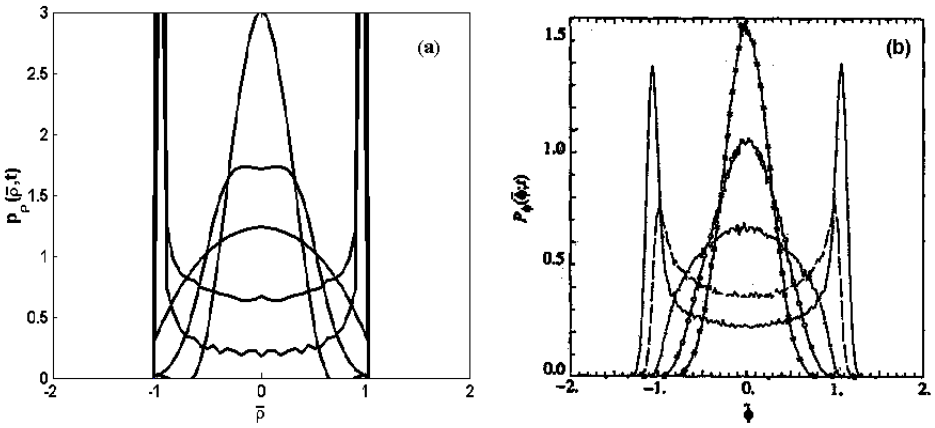

Fig. 3. Pdf evolution of number density in equal mass case. (a) LBE and (b) DNS.[7]

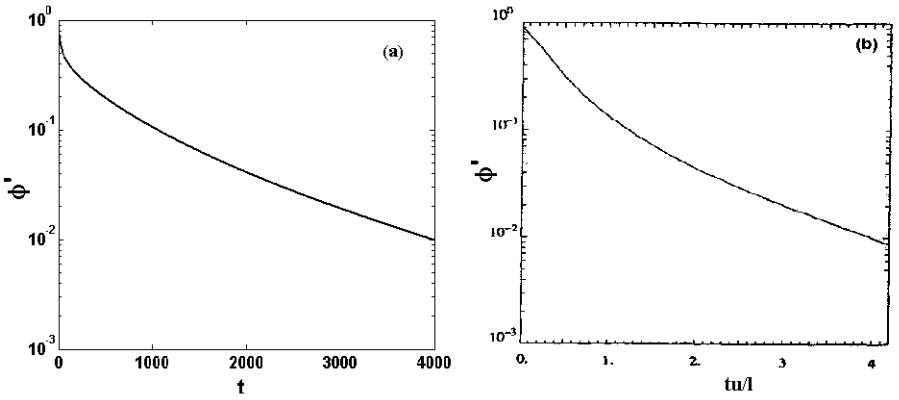

Fig. 4. Evolution of rms scalar (ϕ') in equal mass case. (a) LBE ($\phi' = 2\rho'$) and (b) DNS.

where $\langle\cdot\rangle$ implies volume-averaged value. The relaxation time-constant has been chosen to yield the best agreement. For the optimal time-constant, the agreement is again excellent. In ongoing work, we attempt to accurately characterize the relationship between the time-constant and diffusion coefficient.[14] Here, it suffices to say that given the right time-constant, the LBE captures the DNS behavior well, qualitatively and quantitatively.

Unequal mass case ($m^b = 2.0, m^w = 1.0$)**.** The unequal mass case is particularly interesting since it represents a more practical problem, mixing between species of unequal mass densities. In this case, the initial distribution of black and white species is similar to the equal mass case. Thus the average number density of black and white species are identical. However, the molecular weight of the black

species is twice that of the white species. Hence, the macroscopic mass density of the black species is twice that of the white species. The precise definition of the mass density used here is

$$\overline{\rho^\sigma} = \frac{\rho^\sigma - \rho^\varsigma}{\rho^\sigma + \rho^\varsigma} = \frac{m^\sigma n^\sigma - m^\varsigma n^\varsigma}{m^\sigma n^\sigma + m^\varsigma n^\varsigma}$$

and the particle number density is

$$\overline{n^\sigma} = \frac{n^\sigma - n^\varsigma}{n^\sigma + n^\varsigma}$$

In the unequal molecular weight case, mass density and number density are two

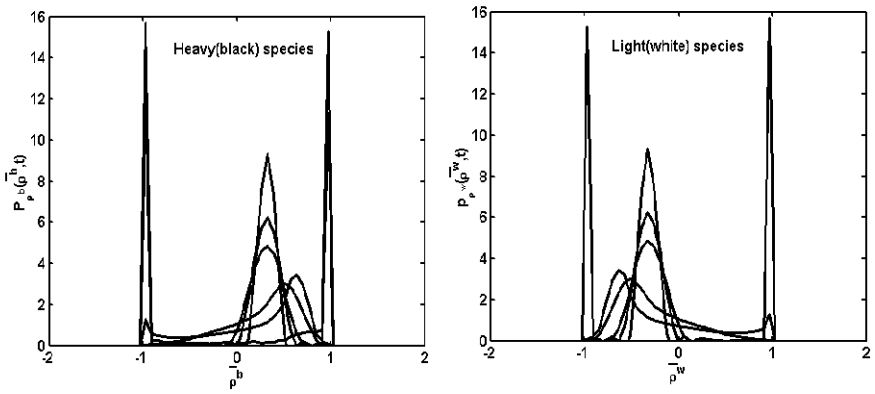

Fig. 5. Pdf evolution of mass density in unequal mass case ($m^b : m^w = 2 : 1$).

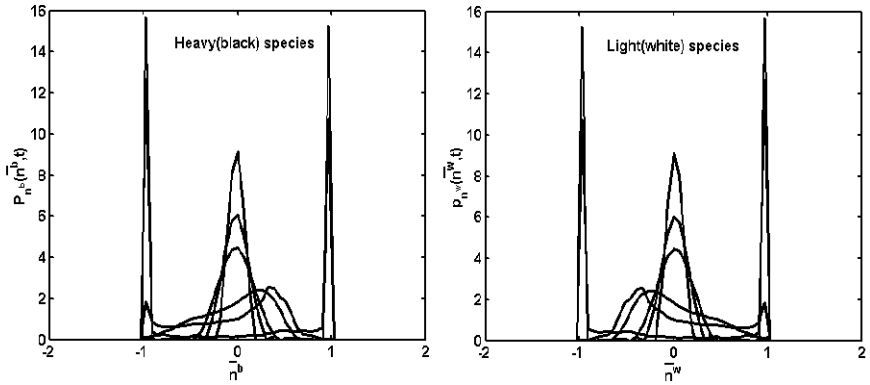

Fig. 6. Pdf evolution of number density in unequal mass case ($m^b : m^w = 2 : 1$).

independent entities. The evolution of both these quantities are investigated. In Figure 5, the mass density evolution is given for both species. The mass density goes from an initial double-delta shape to a Gaussian-like shape centered around the global average of the respective density. The final pdf shape for each species is clearly not symmetric. This is easily understood since the overall average density of the black species is twice that of the white species.

In Figure 6, the number density evolution is shown. Since the average number density is identical for both species, the final pdf distribution is symmetric about the mean value for each species. However, the intermediate forms of the pdf are quite nonsymmetric, demonstrating that the mixing process in this case is quite different from the equal-mass case even if the final distributions are similar. A detailed study of the physics of mixing between species of unequal mass-densities will be undertaken later.

3.2. *Reacting flow in a 1-D channel*

In this example, we study the ability of LBM to simulate chemical reaction. The simplest non-trivial case when reaction can be studied without the complicating effects of mixing is the case of 1-D flame propagation through a homogeneous premixed mixture.

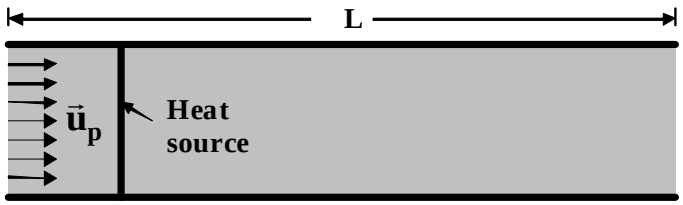

Fig. 7. A schematic illustration of a simple 1-D reacting flow.

Schematic of the flow simulated is shown in Figure 7. For this simple case, the background flow generated from Eq. (18) maintains both the pressure and velocity fields uniform in space and time. A heat source is placed at a location close to the inlet to ignite the mixture. Once ignition is achieved, the heat source is removed. At subsequent times the flame propagates to the right. Initial conditions are set as following:

The values of pressure and velocity are set at $p = 1$, $u_x = u_{in} = 0.1$, $u_y = 0.0$. Both fields are maintained uniform at all times in this simple case. The temperature is set at $T = 300\,^{\circ}K$ everywhere except at $x = 50$ where a heat source is placed with $T_{\text{source}} = 1500\,^{\circ}K$ to ignite the mixture. The hot spot is removed after the mixture ignites. The mass ratio of nitrogen is $Y_{N_2} = 0.7375$. The well-premixed

mixture consists of propane and oxygen with the mass ratios of $Y_{C_3H_8} = 0.2252$, $Y_{O_2} = 0.0373$. The mass fractions of the products are initially set to zero: $Y_{CO_2} = Y_{H_2O} = 0.0$.

Periodic boundary conditions are used at the top and bottom boundaries and the fully developed boundary condition is applied at the outlet. At the inlet, the initial conditions are maintained.

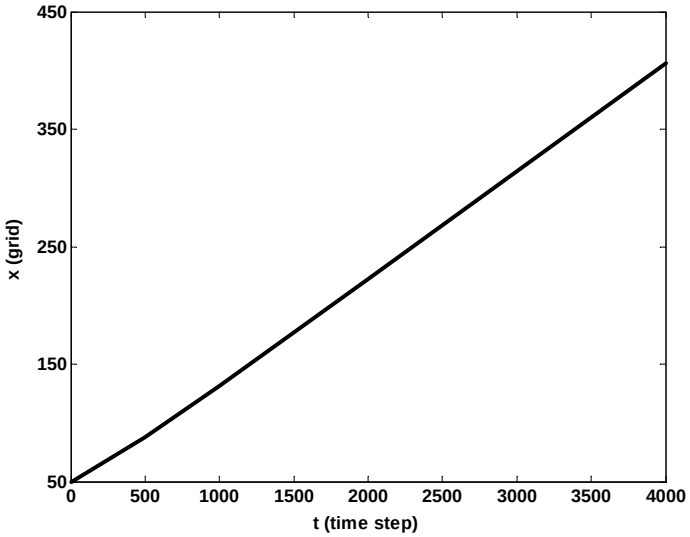

Fig. 8. The flame position evolution with time t.

In Figure 8, the flame position is shown as a function of time. The flame location is identified as the position with the highest reaction rate at any given time. The linear variation of flame location with time (in Figure 8) indicates that the flame propagates at a nearly constant rate. This flame speed can be easily estimated from knowing the flame position at initial ($t_i = 0$; $x_{fl} = 50$) and final ($t_f = 4000$; $x_{fl} = 406$) times. The flame speed thus calculated is

$$v_f = \frac{x_{fl}(t_f) - x_{fl}(t_i)}{t_f - t_i} = \frac{406 - 50}{4000 - 0} = 0.0089$$

in lattice units. Knowing the flame speed, the burning velocity can be easily determined:

$$S_L = u_{\text{in}} - v_f$$

In the above, u_{in} is the reactant velocity at the inlet (which is maintained uniform throughout the flow-field). The burning velocity thus obtained will be in lattice

units. This can be converted into metric units as follows:

$$S_L = \frac{u_{\text{in}} - v_f}{u_{\text{in}}} \cdot u_p \tag{28}$$

The resulting burning velocity is $S_L = 0.11$ [m/s] which compares extremely well with the value obtained from experiments for a propane-air flame.[17]

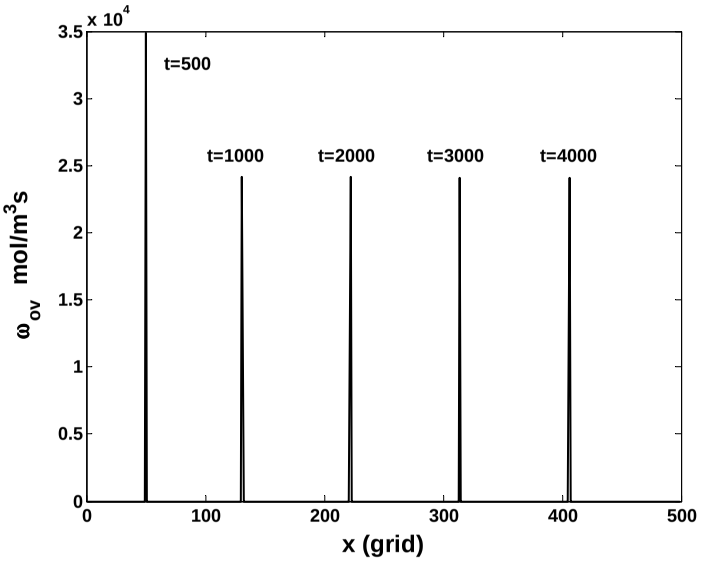

Fig. 9. Reaction rate profiles at different times.

Figure 9 shows that the reaction rate profile in the reaction zone as time evolves. Simulations indicate that flame behavior is sensitive to the magnitude of the heat source.

4. Conclusions

In this paper, we simulate scalar mixing and chemical reacting flows using LBM. In the case of equal-density species mixing, well known results from continuum Navier-stokes simulation are reproduced. The true advantage of the LBM can be seen from the mixing simulations of species of different molecular weights. The results appear quite encouraging. Such simulations are very difficult with continuum based methods. The premixed reacting flow simulations also produce results that are in good agreement with known data. Based on these simulations, we conclude that LBM can perform adequately for more complicated turbulent combustion simulations.

Appendix A. Physical parameters used in the reacting flow simulation

- Reaction coefficient $\kappa_{\rm ov} = 9.9 \times 10^7\ [m^3 \cdot mol^{-1} \cdot s^{-1}]$
- Universal gas constant $R = 8.315\ [J \cdot mol^{-1} \cdot {}^{\circ}K^{-1}]$
- Effective activation energy $E = 30\ [kcal \cdot mol^{-1}] = 1.26 \times 10^5\ [J \cdot mol^{-1}]$
- Heat of overall reaction $Q = 2.05 \times 10^6\ [J \cdot mol^{-1}]$
- Density of pre-mixed mixture $\rho = 1.2\ [kg \cdot m^{-3}]$
- Heat capacity $c_p = 29.1\ [J \cdot mol^{-1} \cdot {}^{\circ}K^{-1}] = 10^3\ [J \cdot kg^{-1} \cdot {}^{\circ}K^{-1}]$
- Kinetic viscosity $\nu = 1.6 \times 10^{-5}\ [m^2 \cdot s^{-1}]$
- Thermal diffusivity $\kappa = 2.2 \times 10^{-5}\ [m^2 \cdot s^{-1}]$
- Diffusivities

$$D_{\rm C_3H_8} = 1.1 \times 10^{-5}\ [m^2 \cdot s^{-1}], \quad D_{\rm O_2} = 2.1 \times 10^{-5}\ [m^2 \cdot s^{-1}]$$
$$D_{\rm CO_2} = 1.6 \times 10^{-5}\ [m^2 \cdot s^{-1}], \quad D_{\rm H_2O} = 2.2 \times 10^{-5}\ [m^2 \cdot s^{-1}]$$

- Mass weight

$$M_{\rm C_3H_8} = 4.4 \times 10^{-2}\ [kg \cdot mol^{-1}], \quad M_{\rm O_2} = 3.2 \times 10^{-2}\ [kg \cdot mol^{-1}]$$
$$M_{\rm CO_2} = 4.4 \times 10^{-2}\ [kg \cdot mol^{-1}], \quad M_{\rm H_2O} = 1.8 \times 10^{-2}\ [kg \cdot mol^{-1}]$$

- Equivalent ratio

$$\phi = \frac{Y_{\rm C_3H_8}/Y_{\rm O_2}}{0.276} = 0.6$$

- Length of the 1-D channel $L = 16.7\ [mm]$
- Physical velocity $u_p = 1.0\ [m \cdot s^{-1}]$

References

1. G. McNamara and G. Zanetti, Use of the Boltzmann equation to simulate lattice-gas automata, *Phys. Rev. Lett.* **61**, 2332 (1988).
2. G. D. Doolen, editor, *Lattice Gas Methods for Partial Differential Equations*, Addison-Wesley, New York, 1990.
3. R. Benzi, S. Succi, and M. Vergassola, The lattice Boltzmann equation: Theory and applications, *Physics Reports* **222**, 145 (1992).
4. X. He and L.-S. Luo, *A priori* derivation of the lattice Boltzmann equation, *Phys. Rev E* **55**, R6333 (1997).
5. X. He and L.-S. Luo, Theory of the lattice Boltzmann method: From the Boltzmann equation to the lattice Boltzmann equation, *Phys. Rev E* **55**, 6811 (1997).
6. X. Shan and X. He, Discretization of the velocity space in the solution of the Boltzmann equation, *Phys. Rev. Lett.* **65**, 65 (1998).
7. D. Wolf-Gladrow, *Lattice-Gas Cellular Automata and Lattice Boltzmann Models*, Springer-Verlag, Heidelberg, 2000.
8. M. Junk, Kinetic schemes in the case of low Mach numbers, *J. Computat. Phys.* **151**, 947 (1999).
9. M. Junk and A. Klar, Discretizations for the incompressible Navier-Stokes equations based on the lattice Boltzmann method, *SIAM J. Scien. Comput.* **22**, 1 (2000).
10. S. Chen and G. Doolen, Lattice Boltzmann method for fluid flows, *Annu. Rev. Fluid Mech.* **30**, 329 (1998).

11. L.-S. Luo, The future of lattice-gas and lattice Boltzmann methods, in *Computational Aerosciences in the 21st Century*, edited by M. D. Salas and W. K. Anderson (Kluwer, Dordrecht, 2000), pp. 165–187.
12. Y. H. Qian, D. d'Humières, and P. Lallemand, Lattice BGK model for Navier-Stokes equation, *Europhys. Lett.* **17**, 479 (1992).
13. H. Chen, S. Chen, and H. W. Matthaeus, Recovery of the Navier-Stokes equation using a lattice Boltzmann method, *Phys. Rev. A* **15**, R5339 (1992).
14. L.-S. Luo, H. D. Yu, and S. Girimaji, Binary mixing simulations using lattice Boltzmann method, in preparation.
15. K. Yamamoto, X. He, and G. D. Doolen, Simulation of combustion field with lattice Boltzmann method, *J. Stat. Phys.* **107**, 367 (2002).
16. V. Eswaran and S. B. Pope, Direct numerical simulations of the turbulent mixing of a passive scalar, *Phys. Fluids* **31**, 506 (1988).
17. I. Yamaoka and H. Tsuji, in *Twentieth International Symposium Combustion* (The Combustion Institute, Pittsburgh, 1982), pp. 1883.